SETAC PRESS

INDIRECT PHOTOCHEMICAL TRANSFORMATIONS OF ACYCLOVIR AND PENCICLOVIR IN AQUATIC ENVIRONMENTS INCREASE ECOLOGICAL RISK

JIBIN AN,†‡ GUIYING LI,† TAICHENG AN,*† and XIANGPING NIE§
†State Key Laboratory of Organic Geochemistry and Guangdong Key Laboratory of Environmental Resources Utilization and Protection,
Guangzhou Institute of Geochemistry, Chinese Academy of Sciences, Guangzhou, People's Republic of China
‡University of Chinese Academy of Sciences, Beijing, People's Republic of China
§Institute of Hydrobiology, Jinan University, Guangzhou, People's Republic of China

Abstract: Acyclovir and penciclovir, 2 antiviral drugs, are increasingly detected in aquatic environments. The present study explores the natural photochemical transformation mechanisms and fate of these drugs, examining direct and indirect photochemical transformation under simulated sunlight irradiation. The 2 antiviral drugs are photostable under certain conditions but significantly degrade in the presence of chromophoric dissolved organic matter (DOM). The degradation rate associated with the drugs' indirect photochemical transformation scaled with chromophoric DOM concentration. Quenchers and sensitizers were used to identify indirect photochemical transformation mechanism. Results suggested that both pharmaceuticals could be transformed by reacting with $^1O_2$, $^\bullet OH$, and excited chromophoric DOM. The $^1O_2$ played an important role in indirect photochemical transformation. Furthermore, the reaction kinetics between their substructural molecules, guanine, isocytosine, and imidazole, with different reactive oxygen species were evaluated to determine which substrate functionalities were most susceptible to singlet oxygenation. Imidazole was identified as the reaction site for $^1O_2$, and preliminary $^1O_2$ oxidation mechanisms were further evaluated based on liquid chromatographic–tandem mass spectrometric results. Finally, aquatic ecotoxicity assessment of phototransformed solutions revealed that the degradation of acyclovir and penciclovir may not ultimately diminish environmental risk because of either formation of more toxic intermediates than parent pharmaceuticals or some synergistic effects existing between the intermediates. *Environ Toxicol Chem* 2016;35:584–592. © 2015 SETAC

INTRODUCTION

Various pharmaceuticals are well-known emerging organic contaminants in natural aquatic environments, although concentrations are at trace levels, and pose adverse effects to aquatic ecosystems and public health [1–4]. Along with other pharmaceuticals and personal care products, antiviral drugs are found frequently in wastewater-treatment plant effluents as well as surface water [5,6]. Two important antiviral drugs, acyclovir and penciclovir, used to treat herpes infections [7], are frequently detected in water environments at the nanogram per liter level [5]. However, information about the environmental transformation process of acyclovir and penciclovir in water is limited. Prasse et al. [8] reported biotransformation of acyclovir and penciclovir with activated sludge and found a biodegradation half-life of 5.3 h. This points to the rapid removal of the pharmaceutical substances using conventional wastewater-treatment technology. However, a derivative biorefractory product, carboxyl-acyclovir, persisted longer than the test, at 29 d [8]. Moreover, several penciclovir biotransformation products are likely to be ecotoxicologically relevant because of aldehyde functional groups at the molecular level, such as the α,β-unsaturated aldehydes glyoxal and malondialdehyde. These aldehydes may lead to enzyme inactivation or even interact with DNA macromolecules [8–10]. Thus, studying environmental transformation mechanisms and the ecotoxicity evolution of these 2 emerging organic

contaminants, as well as their transformation products in natural water environments, is of great importance.

Natural transformation processes, such as solar-driven photochemical transformation, likely play an important role in the environmental fate of emerging organic contaminants, including direct and indirect photochemical degradation reactions [11–13]. In direct photochemical transformation processes, compounds absorb radiation and undergo chemical changes, whereas in indirect photochemical transformation processes, chromophoric dissolved organic matter (DOM)—the light-absorbing (ultraviolet and visible [UV-vis]) fraction of dissolved organic carbon—acts as a sensitizer absorbing irradiation and leads to the formation of reactive oxygen species (ROS), such as hydroxyl radical ($^\bullet OH$), singlet oxygen ($^1O_2$), hydrogen peroxide (H_2O_2), perhydroxyl radical ($HOO^\bullet$), superoxide radical ($O_2^{\bullet-}$), as well as excited state triplet chromophoric DOM, subsequently initiating chemical degradation by these ROS [14,15]. Although the steady-state concentrations of these ROS are at micro-scales in natural waters (e.g., 10^{-19} to 10^{-9} M), levels are sufficient to facilitate aquatic organic contaminant transformation [16]. In particular, $^\bullet OH$, $^1O_2$, and excited state triplet chromophoric DOM are primary ROS contributing to organic pollutant elimination in sunlight, activating chromophoric DOM [17,18]. On the other hand, the chromophoric DOM in water may slow organic pollutant removal because of the light screening effect (fewer photons reach the organic pollutant) [19]. Therefore, chromophoric DOM may play a significant role in the photochemical transformation of organic pollutants, especially emerging organic contaminants, depending on the magnitude of these 2 factors [20,21]. Furthermore, photochemical degradation of organics does not guarantee complete decontamination because of toxic product formation [22,23]. As such, identifying

photochemical degradation intermediates and evaluating treated solution ecotoxicity are necessary because despite low concentrations, some synergistic or antagonistic effects may occur in photoproduct mixtures [24].

To our knowledge, little research about the natural photochemical transformation fate of acyclovir and penciclovir in water environments has been completed. Since both pharmaceuticals lack the potential of direct photolysis because of minimal overlap between the UV-vis absorption spectrum and the incident sunlight's emission spectrum in the 290 to 800 nm wavelength range, these are anticipated to be photostable in aquatic environments.

Thus, the main purpose of the present study was to characterize the indirect photochemical transformation mechanisms of antiviral drugs in water environments. Two antiviral drugs, acyclovir and penciclovir, and their substructural subunits, guanine, isocytosine, and imidazole, were chosen as model compounds (Figure 1). Fulvic acid extracted from weathered coal was used as a proxy for chromophoric DOM [25]. To better understand the photochemical transformation mechanism, quenching and kinetic solvent isotope experiments were performed to assess the contribution of various ROS. In addition, photochemical degradation products were identified using ultra-performance liquid chromatography–tandem mass spectrometry (UPLC-MS/MS) with electrospray ionization and verified by the reaction between the drug's 3 substructural subunits and ROS. Finally, the aquatic ecotoxicity of acyclovir and penciclovir, as well as their indirect photochemical transformation solutions, were also assessed in detail at 3 different aquatic organism trophic levels: *Photobacterium phosphoreum*, *Selenastrum capricornutum*, and *Daphnia magna*.

MATERIALS AND METHODS

Materials

Acyclovir and penciclovir ($\geq$99% purity) were purchased from Tokyo Chemical Industry. Guanine, isocytosine, imidazole, terephthalic acid, 2-hydroxyterephthalic acid (2HO-terephthalic acid), furfural alcohol, furan-2-carbaldehyde, acetophenone, and rose bengal ($C_{20}H_2Cl_4I_4Na_2O_5$) were all purchased from Sigma-Aldrich ($\geq$99% purity) and used as received. The luminescent bacterium *P. phosphoreum* was purchased form the Institute of Soil Science, Chinese Academy of Sciences.
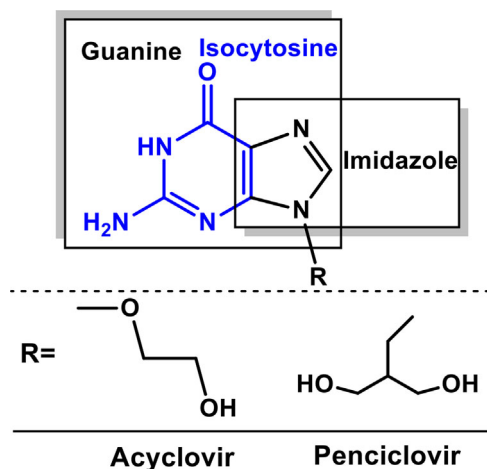

Figure 1. Structures of acyclovir, penciclovir, and its substructural moieties, guanine, isocytosine, and imidazole.

Selenastrum capricornutum and monoclonal *D. magna* were provided by the Institute of Hydrobiology, Jinan University, China. Fulvic acid (C 54.82%, H 2.29%, O 41.14%, N 0.66%, and S 1.09%) extracted from weathered coal was purchased from Pingxiang Red Land Humic Acid. Deionized water was obtained using the Millipore Milli-Q system. All other chemicals were of analytical reagent–grade.

Photochemistry procedures

Photochemical transformation experiments were conducted using a 150-W Xenon Short Arc Lamp (Zolix). Appropriate glass filters were used to restrict the transmission of irradiation wavelengths less than 290 nm, resulting in a wavelength spectrum similar to natural solar light (light intensities are provided in Supplemental Data, Figure S1). The emission spectra of the lamps were measured using an Ocean Optics USB2000+ UV-vis spectrophotometer and normalized according to the actinometry results, considering the absorbance of Pyrex glass walls of the irradiation cells. Samples were photolyzed in a capped cylindrical Pyrex vessel (27.5 mm inner diameter) with a screw cap. The cylindrical vessels were placed at 5 cm in front of the lamp, filled with 25 mL of the test solution, and maintained at 25 °C using cooling water.

Direct photochemical transformation experiments were conducted in 10.0 mM phosphate buffer solutions at pH values of 5.0, 7.0, and 9.0; indirect photochemical transformation experiments were conducted in buffered distilled water with 20 mg L^{-1} of fulvic acid. Several scavengers were added to the fulvic acid–enriched samples to investigate the indirect photochemical transformation mechanism. Deoxygenated samples were bubbled with nitrogen gas for 20 min to inhibit $^1O_2$ formation and enhance excited fulvic acid formation. Because of differences in $^1O_2$ quenching rates by deuterium oxide (D$_2$O) and H$_2$O, kinetic solvent isotope effect experiments were done to discern $^1O_2$ involvement. The fulvic acid–enriched solution contained 90% D$_2$O, rather than straight H$_2$O, for these tests so that if indirect photochemical transformations were involved in the $^1O_2$ reaction, the reaction would proceed more rapidly in the deuterated solvent.

Determining reaction rates and steady-state concentrations of $^1O_2$ or $^{\bullet}OH$

A competition kinetic method was used to determine the bimolecular rate constant of acyclovir or penciclovir with $^1O_2$ or $^{\bullet}OH$. Rose bengal was used as the photosensitizer to produce $^1O_2$. A solution containing 100 μM acyclovir or penciclovir, 200 μM furan-2-carbaldehyde (reference compound), and 50 μM rose bengal in a pH 7.0 phosphate buffer was exposed to a solar simulator. Thermal $^1O_2$ generation was used to determine the bimolecular rate constant of acyclovir or penciclovir with $^1O_2$. That is, $^1O_2$ was generated in the absence of light from the reaction between MoO$_4^{2-}$ and H$_2$O$_2$ [18]. We added H$_2$O$_2$ (200 μM) to buffered solutions containing acyclovir or penciclovir (100 μM), MoO$_4^{2-}$ (1 mM), and furan-2-carbaldehyde (200 μM). Samples of 375 μL were withdrawn at set intervals, immediately quenched with 125 μL of sodium azide (500 μM) solution, and then analyzed using high-performance liquid chromatography (HPLC). To determine the bimolecular reaction rate constants of $^{\bullet}OH$ with the acyclovir or penciclovir, Fenton's reagent (40 μM FeSO$_4 \times$ 7H$_2$O and 1 mM H$_2$O$_2$) was added into different solutions containing the acyclovir or penciclovir and 20 μM acetophenone as a reference compound [26]. The pH value of solutions was adjusted to 3 with perchloric acid. Samples

(0.5 mL) were withdrawn at set intervals, quenched using 0.5 mL methanol, and analyzed using HPLC. The bimolecular rate constants of the acyclovir or penciclovir with $^1O_2$ or $^\bullet OH$ were determined by comparing acyclovir or penciclovir (Substrate) degradation against the reference compound degradation. This is shown in Equation 1, where $k_{1_{O_2, FAD}} = 8.4 \times 10^4 \, M^{-1} \, s^{-1}$ [27], $k_{\cdot OH, acet} = 5.9 \times 10^9 \, M^{-1} \, s^{-1}$ [26].

$$k_{1_{O_2}/\cdot OH,S} = \frac{\ln\left([Substrate]_t/[Substrate]_o\right)}{\ln\left([Reference]_t/[Reference]_o\right)} k_{1_{O_2}/\cdot OH,R} \quad (1)$$

Steady-state concentrations of $[^1O_2]_{ss}$ and $[^\bullet OH]_{ss}$ in chromophoric DOM–enriched water were determined under simulated sunlight irradiation. To determine $[^1O_2]_{ss}$, a solution containing $20 \, mg \, L^{-1}$ fulvic acid and furfural alcohol ($200 \, \mu M$, a common $^1O_2$ probe) was irradiated with simulated sunlight. The steady-state concentration of $^1O_2$ was determined using Equation 2 [27]

$$\frac{d[FFA]}{dt} = -k_{1_{O_2, FFA}}[FFA]\,[^1O_2]_{ss} \quad (2)$$

where FFA is furfural alcohol and $k_{1_{O_2, FFA}} = 8.3 \times 10^7 \, M^{-1} \, s^{-1}$.

To determine $[^\bullet OH]_{ss}$, a solution containing $20 \, mg \, L^{-1}$ fulvic acid and terephthalic acid ($200 \, \mu M$) was used. Under simulated sunlight irradiation, terephthalic acid hydroxylation was conducted to form 2HO-terephthalic acid, with a 35% reaction yield. The observed 2HO-terephthalic acid formation rate was used to calculate $^\bullet OH$ concentration with Equation 3 [28].

$$\frac{d[2HO - TPA]}{dt} = 0.35 \times k_{\cdot OH, TPA}[TPA][\cdot OH]_{ss} \quad (3)$$

where $k_{\cdot OH, TPA} = 3.3 \times 10^9 \, M^{-1} \, s^{-1}$.

To further investigate whether acyclovir or penciclovir alone produce $^1O_2$ or $^\bullet OH$, a 50-μM acyclovir or penciclovir with $200 \, \mu M$ furan-2-carbaldehyde or $200 \, \mu M$ terephthalic acid, solution was irradiated in simulated sunlight for 2 h; samples were withdrawn every 20 min for analysis.

Analysis procedures

HPLC. Acyclovir and penciclovir concentrations were analyzed using an Agilent 1200 series HPLC system under the following conditions. The analysis was performed with a Kromasil C18 column ($250 \times 4.6 \, mm$, $5 \, \mu m$ particle size) at $25 \, ^\circ C$. The mobile phase was the mixture of 90% water and 10% methanol (by volume) at a flow rate of $1 \, mL \, min^{-1}$ [29]. The detection wavelength was $254 \, nm$, and the injection volume was $20 \, \mu L$. The HPLC mobile phase for the detection of terephthalic acid and 2HO-terephthalic acid was 60% phosphate buffer (pH 3) and 40% methanol at a flow rate of $1 \, mL \, min^{-1}$ at $25 \, ^\circ C$. Ultraviolet detection was used at $225 \, nm$ for terephthalic acid, and fluorescence detection was used for 2HO-terephthalic acid with excitation at $250 \, nm$ and emission at $410 \, nm$. The HPLC mobile phase for the detection of furan-2-carbaldehyde ($274 \, nm$) and furfural alcohol (UV $218 \, nm$) was 45% water and 65% methanol at a flow rate of $1 \, mL \, min^{-1}$ at $25 \, ^\circ C$.

UPLC/MS/MS. We used UPLC/MS/MS (Waters XevoTQ; Micromass MS Technologies) to identify degradation products. Samples were separated using an Acquity HPLC BEH C18 column ($2.1 \times 100 \, mm$, particle diameter of $1.7 \, \mu m$) with mobile phases of 10% methanol and 90% formic acid solution

(5 mM) at a flow rate of $0.2 \, mL \, min^{-1}$. The MS was operated in negative electrospray ionization mode. The source temperature was set at $150 \, ^\circ C$; argon was used as a collision gas with different collision energies for daughter ion analysis. The desolvation temperature was $350 \, ^\circ C$; N_2 was used as a desolvation gas with a flow rate of $650 \, L \, h^{-1}$.

Aquatic ecotoxicity assay

The initial concentration of $100 \, \mu M$ acyclovir or penciclovir was used to estimate the acute toxicity of acyclovir or penciclovir and their intermediates during a singlet oxygen oxidation process. The ecotoxicity of the treated acyclovir or penciclovir solution was evaluated using organisms at 3 different trophic levels: *P. phosphoreum*, *S. capricornutum*, and *D. magna*. In 3 sets of experiments, 2, 27, and 44 mL of the degradation solution or pure water (control) were used; and results were normalized against the control as percentages. For the toxicity bioassay with *P. phosphoreum*, the assays were carried out according to the standardized GB/T 15441-1995, and the standard procedure was employed to reconstitute the bacteria, using sodium chloride solution. Luminescence was determined with a Luminometer DXY-3 (Institute of Soil Science, Chinese Academy of Sciences), and toxicity was determined after 15-min incubation [23,29]. The *S. capricornutum* bioassay was carried out according to the Organisation for Economic Co-operation and Development guideline for algal growth inhibition test 201, and the algal biomass at different exposure times was measured by manual cell counting using a microscope. For the toxicity bioassay with *D. magna*, each sample contained 10 individuals, and each assay was performed in triplicate. The toxicological endpoint was immobilization after 24-h and 48-h exposure to an experimental medium containing $220 \, mg \, L^{-1}$ $CaCl_2$, $60 \, mg \, L^{-1}$ $MgSO_4$, $65 \, mg \, L^{-1}$ $NaHCO_3$, and $6 \, mg \, L^{-1}$ KCl. The definition of "immobilization" was that daphnia were not able to swim within 15 s after gentle agitation of the test vessel (even if they could still move their antennae). All experiments were repeated independently 3 times.

Statistical analysis

Statistical significance was determined using the Student 2-tailed *t* test. Analysis of variance was used for multiple comparisons. Differences between groups were considered significant at $p \leq 0.05$.

RESULTS AND DISCUSSION

Photochemical transformation kinetics

There are 2 types of emerging organic contaminant photochemical transformations in water, direct and indirect. Direct photochemical transformation occurs when the substrates themselves absorb light and undergo subsequent photochemical transformation. Indirect photochemical transformation occurs when excited photosensitizers mediate substrate transformation. Many studies have reported that the photochemical degradation of organics in aquatic environments follow first-order kinetics [30–32]. Substrate loss follows the generic rate law in Equation 4

$$\frac{-d[Substrate]}{dt} = \left(k_{direct} + \sum k_{ROS}[33]\right) + [Substrate] \quad (4)$$

where k_{direct} is the observed first order rate constant for direct photolysis and k_{ROS} is the bimolecular rate constant for the ROS reaction with substrate. Supplemental Data, Figures S1 and S2, show the UV-vis absorption spectra and direct photochemical transformation kinetics of acyclovir and penciclovir at different pH values. The results showed that 2 drugs displayed minimal overlap between their UV-vis absorption spectrum and the emission spectrum of simulated sunlight irradiation. As such, these are demonstrated to be photostable across all investigated pH values. Furthermore, when pH increased, the red-shifted absorption spectra were not observed for acyclovir and penciclovir, indicating that direct photochemical transformation was impossible for both the protonation and deprotonation states of 2 substrates under simulated sunlight irradiation. However, adding fulvic acid $(10\text{--}40\,\text{mg L}^{-1})$ in the acyclovir or penciclovir solution significantly enhanced photochemical transformation (Figure 2). These results indicated that simulated sunlight irradiation enables acyclovir or penciclovir indirect photochemical transformations. Thus, the k_{direct} term in Equation 4 can be ignored completely, leading to the acyclovir and penciclovir indirect photochemical transformation kinetics model in Equation 5

$$-\frac{d[\text{Substrate}]}{dt} = \sum k_{ROS}\,[\text{ROS}]\,[\text{Substrate}]$$
$$= \Big(k_{\cdot OH}[\cdot OH] + k_{1_{O_2}}[^1O_2] + k_{FA\cdot}[FA\cdot] + k_{O_2^-}[O_2^{\cdot-}]$$
$$+ k_{other}\Big)[\text{Substrate}] \tag{5}$$

where $k_{\cdot OH}$, $k_{1_{O_2}}$, and $k_{FA\cdot}$ are the bimolecular rate constants for the $\cdot OH$, $^1O_2$ reaction and excited state of fulvic acid with the substrates, respectively; k_{other} is the first-order rate constant for other concurrent degradation processes. Figure 3 depicts the indirect photochemical transformation processes of acyclovir and penciclovir in fulvic acid–enriched water under simulated sunlight irradiation. Because direct photochemical transformation cannot occur under simulated sunlight irradiation, we thoroughly evaluated the indirect photochemical transformation mechanism, as well as the acyclovir and penciclovir degradation pathways.
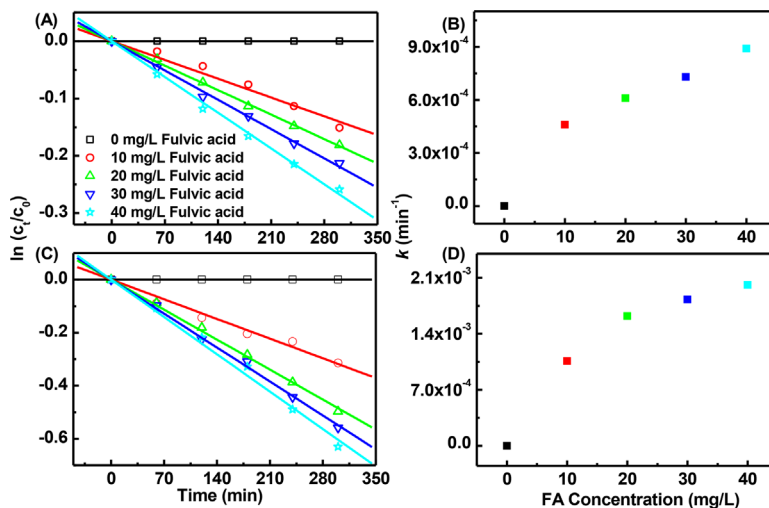
a FA is fulvic acid; FA* is excited state singlet FA; isc is inter system crossing; ^{3}FA is excited state triplet FA; O_2 is ground state oxygen; $^1O_2$ is excited state singlet oxygen
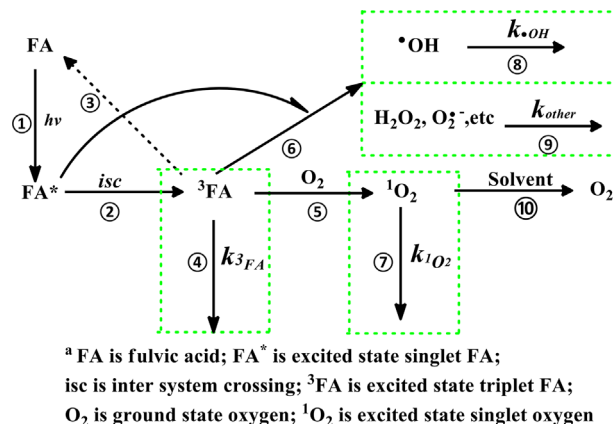
Figure 3. Fulvic acid–mediated possible reaction pathway for indirect photochemical degradation of acyclovir or penciclovir. FA = fulvic acid; FA* = excited state singlet fulvic acid; ^{3}FA = excited state triplet fulvic acid; isc = intersystem crossing; k = rate constant.

The role of ROS

Based on the fulvic acid excited mechanism discussed above, $^1O_2$, $\cdot OH$, $O_2^{\cdot-}$, H_2O_2, and excited state triplet fulvic acid may be important ROS involved in indirect photochemical degradation of acyclovir or penciclovir. As such, several scavenging experiments were conducted to determine which ROS was mainly responsible for indirect photochemical transformation and which pathway was important in Figure 3. Before carrying out these experiments, we directly added $O_2^{\cdot-}$ and H_2O_2 to the acyclovir or penciclovir solutions and determined that the substrates have negligible reactivity toward both ROS (Supplemental Data, Figure S3). Corresponding results of other ROS quenching experiments are shown in Supplemental Data, Figure S4. When no scavengers were added, the highest indirect photochemical degradation rates for both acyclovir and penciclovir were achieved in the pure fulvic acid–enriched water, which is the collective effect of all ROSs. When different scavengers were added, the degradation rates for both drugs decreased to a certain extent. For example, the $^1O_2$ quencher sodium azide (1.5 mM) had the largest impact on indirect photochemical acyclovir and penciclovir degradation rates,

Figure 2. Photochemical transformation kinetics of 2 μM acyclovir in the presence of fulvic acid (**A**). Effect of fulvic acid concentration on the photochemical transformation rate constant of acyclovir (**B**). Photochemical transformation kinetics of 2 μM penciclovir in the presence of fulvic acid (**C**). Effect of fulvic acid concentration on the photochemical transformation rate constant of penciclovir (**D**). FA = fulvic acid.

followed by the •OH quencher (0.1 M isopropanol). The excited fulvic acid had little effect on the indirect photochemical degradation rates, which is revealed by adding 0.1 M isopropanol and 1.5 mM sodium azide to quench both •OH and $^1O_2$. These results suggest that $^1O_2$ is the most important ROS involved in the indirect photochemical acyclovir and penciclovir degradation in natural water environments. Therefore, experiments were designed to confirm $^1O_2$ involvement in the photochemical transformation of acyclovir or penciclovir in fulvic acid–enriched water. As known, $^1O_2$ has a longer life in D_2O solutions than in H_2O. As such, reaction solutions containing D_2O will accelerate the reaction rates if the $^1O_2$ is involved in the reactions because the reactions in 100% D_2O will proceed approximately 14 times faster than in 100% H_2O [33,34]. Thus, kinetic solvent isotope effect experiments were also conducted to confirm $^1O_2$ involvement in the photochemical degradation process. The expected kinetic solvent isotope effects were calculated at the mole fractions (χ) of D_2O and H_2O using Equation 6.

$$\frac{k_{obs,D_2O\ mix}}{k_{obs,H_2O}} = \frac{k_{H_2O}}{x_{H_2O}k_{H_2O} + x_{D_2O}k_{D_2O}} \qquad (6)$$

Reaction solutions containing 90% D_2O were created; the expected kinetic solvent isotope effect is obtained approximately 7 times at this solvent ratio. Figure 4 shows the corresponding results, which show that photochemical degradation of acyclovir or penciclovir in 90% D_2O was more clearly augmented than in the 100% H_2O reaction solutions. However, the reaction rate constant was not at the expected level. Besides $^1O_2$, other ROS such as •OH or excited fulvic acid may also be involved in the photochemical degradation of acyclovir or penciclovir in fulvic acid–enriched water. To further assess the relative importance of $^1O_2$, we sparged N_2 into the reaction solution to remove O_2, dramatically decrease the formation of $^1O_2$, and generate a higher steady-state concentration of excited fulvic acid. As Figure 4 shows, the acyclovir or penciclovir

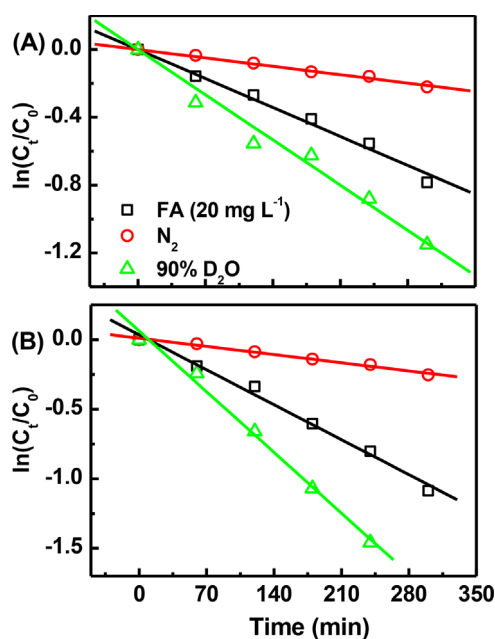elimination rates in the N_2 sparged system were more inhibited than in the air saturation system. This indicates that acyclovir and penciclovir reacted with $^1O_2$ and excited fulvic acid, but excited fulvic acid has a relatively weak reactivity with substrates.

Further experiments focused on determining different ROS contributions to indirect photochemical degradation of acyclovir or penciclovir. In general, the k_{obs} decrease resulting from ROS quenching was assumed to be equivalent to ROS contribution to the overall photochemical degradation. Isopropanol was assumed to quench •OH [35], sodium azide was assumed to quench $^1O_2$ [18], and both isopropanol and sodium azide were assumed to quench •OH and $^1O_2$ [36]. Therefore, the following equations were used to calculate different ROS contributions

$$k_{1_{O_2}}[^1O_2]_{ss} \approx k_{obs} - k_{obs,azide} \qquad (7)$$

$$k_{\cdot OH}[\cdot OH]_{ss} \approx k_{obs} - k_{obs,isopropanol} \qquad (8)$$

$$k_{FA^*}[FA^*]_{ss} \approx k_{obs,isopropanol} - (k_{obs} - k_{obs,azide}) \qquad (9)$$

where k_{obs}, $k_{obs,azide}$, and $k_{obs,isopropanol}$ were the observed photochemical transformation rate constants in fulvic acid–enriched water with no quenchers, isopropanol and sodium azide, respectively. The validity of these approximations was checked using the predicted ROS contributions; the rate was calculated by multiplying the determined bimolecular reaction rate constant by the measured ROS steady-state concentrations. (A summary of the available bimolecular reaction rate constants for the acyclovir or penciclovir reaction with the interested ROS is given in Supplemental Data, Table S1.) Supplemental Data, Table S2, shows the calculated reaction rate of $^1O_2$ and •OH as 9.4×10^{-6} and 8.3×10^{-7} s^{-1} for acyclovir and 3.5×10^{-5} and 7.7×10^{-6} s^{-1} for penciclovir, respectively. The predicted reaction rates of $^1O_2$ and •OH were 8.7×10^{-6} and 9.1×10^{-7} s^{-1} for acyclovir and 1.7×10^{-6} and 6.9×10^{-6} s^{-1} for penciclovir, respectively. The calculated and predicted contributions of $^1O_2$ and •OH were within ±10% agreement of each other, suggesting that the quenching experiment is a rational way to evaluate different ROS contributions. As Figure 5 shows, indirect photochemical transformation induced by $^1O_2$ was the main elimination process, rather than •OH or the excited state of fulvic acid. The $^1O_2$ had a contribution ratio of 91.3% and 84.0% for acyclovir and penciclovir, respectively,

Figure 4. Effect of isotope solvent and dissolved gas on the rate of photochemical transformation of acyclovir (**A**) and penciclovir (**B**) in fulvic acid–enriched water. D_2O = deuterium oxide; FA = fulvic acid.
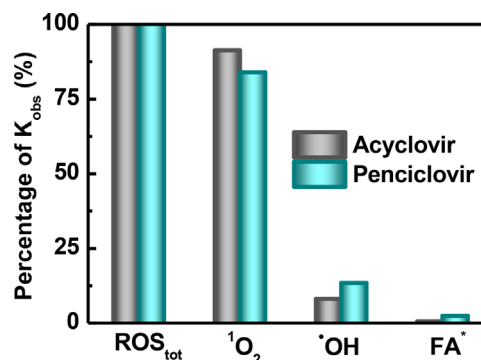

Figure 5. Percentage contribution of singlet oxygen, hydroxyl radical, excited chromophoric dissolved organic matter and other processes to the photochemical transformation of acyclovir and penciclovir in fulvic acid–enriched water under simulated sunlight irradiation. FA = fulvic acid; ROS_{tot} = total reactive oxygen species.

followed by $^{\bullet}$OH with 8.1% and 13.4% and then excited fulvic acid with less than 0.6% and 2.4%, respectively.

Singlet oxygen reaction with acyclovir and penciclovir

The results above show that $^1O_2$ was the most important ROS in the indirect photochemical degradation of acyclovir and penciclovir. As such, the reaction of substrates with $^1O_2$ was also conducted, and pH dependence was measured in 2 $^1O_2$ generation systems (light-irradiated rose bengal and MoO_4^{2-}/H_2O_2 reaction). The dissociation constant values were 2.2 and 9.4 for acyclovir and 3.2 and 9.4 for penciclovir, respectively [5]. Adjusting the pH value of the solution to 5.0, 7.0, 9.0, and 10.0 creates a positive charge or neutral form in the substrate; a pH value of 5.0 was chosen as the lowest pH value because of low rose bengal solubility in acidic conditions. As Table 1 shows, when pH increased from 5.0 to 10.0, the positive charge of acyclovir (χ_1) decreased from 9.98×10^{-1} to 2.01×10^{-2}; the neutral form (χ_0) increased from 3.97×10^{-5} to 7.99×10^{-1}. The bimolecular reaction rate constant for $^1O_2$ reaction with acyclovir also increased from $(2.18 \pm 0.16) \times 10^6$ to $(15.8 \pm 2.00) \times 10^6\,M^{-1}\,s^{-1}$ with the increase of pH from 5.0 to 10.0. The rate constant at pH 10.0 was 5 to 7 times higher than that at pH 5.0 in both systems (light-irradiated rose bengal and MoO_4^{2-}/H_2O_2 reaction). This is mainly because electrophilic $^1O_2$ reacts more quickly with electron-rich deprotonated substrates [37]. Similar results were obtained for the penciclovir reaction with $^1O_2$. The bimolecular reaction rate increased from $(2.60 \pm 0.05) \times 10^6$ at pH 5.0 to $(25.2 \pm 2.98) \times 10^6\,M^{-1}\,s^{-1}$ at pH 10.0. However, the determined rate constants for both

acyclovir and penciclovir in the light-irradiated rose bengal system were higher than in the MoO_4^{2-}/H_2O_2 system. The difference in the rate constants obtained by the 2 systems indicate that the excited rose bengal may also react with the substrates, generating elevated rate constants.

Determination of reaction site and dominated degradation pathway

To gain insights about which is the reaction site of acyclovir or penciclovir with $^1O_2$, 3 submodel function group compounds, guanine, isocytosine, and imidazole, were employed individually to determine their bimolecular reaction rates with $^1O_2$ in MoO_4^{2-}/H_2O_2 solution. As Table 2 shows, imidazole showed similar scale rate constants as acyclovir and penciclovir (1.39 times), strongly pointing to the imidazole ring as the most reactive function group toward $^1O_2$ within the original compounds. Imidazole was approximately 70 times faster than the isocytosine group, indicating that isocytosine was not the main reactive function group within acyclovir and penciclovir molecules. Further, the rate constant of imidazole was also faster than guanine by 42%, suggesting that the electron-withdrawal effect of the carbonyl or nitride group slightly depresses the $^1O_2$ and guanine reaction rate. This was further demonstrated and confirmed at different protonation states at pH 5 to 10. When the guanine ring is protonated, the electron density was reduced and the reactivity toward $^1O_2$ decreased. Nevertheless, because of the electron-withdrawal effect of the acyclovir molecule's ether structure, the bimolecular reaction rate constant becomes much slower than penciclovir, and penciclovir containing electron-donating

Table 1. Singlet oxygen bimolecular rate constants for acyclovir and penciclovir

pH	χ_2	χ_1	χ_0	$K_{rxn}\,^1O_2\,^{a,c}$	$K_{rxn}\,^1O_2\,^{b,c}$	$k_{rel}\,^d$
Acyclovir						
				—	—	—
5.0	1.58×10^{-3}	9.98×10^{-1}	3.97×10^{-5}	2.18 ± 0.16	ND	—
7.0	1.58×10^{-5}	9.96×10^{-1}	3.97×10^{-3}	3.50 ± 0.05	2.70 ± 0.05	1.3
9.0	1.13×10^{-7}	7.15×10^{-1}	2.85×10^{-1}	16.0 ± 1.31	8.63 ± 0.38	1.9
10.0	3.18×10^{-9}	2.01×10^{-2}	7.99×10^{-1}	15.8 ± 2.00	11.3 ± 0.96	1.4
Penciclovir						
				—	—	—
5.0	1.56×10^{-2}	9.84×10^{-1}	4.93×10^{-5}	2.60 ± 0.05	ND	—
7.0	1.58×10^{-4}	9.95×10^{-1}	4.99×10^{-3}	3.95 ± 0.22	0.550 ± 0.01	7.2
9.0	1.06×10^{-6}	6.66×10^{-1}	3.34×10^{-1}	15.1 ± 1.53	17.6 ± 2.17	0.86
10.0	2.64×10^{-8}	1.66×10^{-2}	8.34×10^{-1}	25.2 ± 2.98	18.3 ± 2.64	11.4

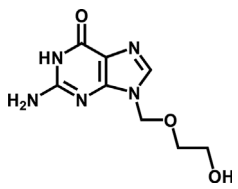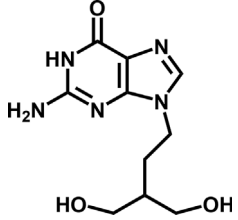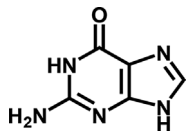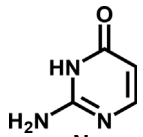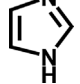[a] Values determined from rose bengal–sensitized photoreaction and furan-2-carbaldehyde probe.
[b] Values determined from molybdate/peroxide reaction and furan-2-carbaldehyde probe.
[c] $10^6\,M^{-1}\,s^{-1}$.
[d] $k_{rel} = k_{RB}/k_{molybdate}$ (k_{rel} = rate constant for the substrates relative to acyclovir; RB = rose bengal).
ND = not detected.

Table 2. Bimolecular rate constants for interaction of $^1O_2$ with acyclovir and penciclovir as well as model compounds

Substrate	Structure	k (M^{-1}s^{-1})	k_{rel}[a]
Acyclovir		$(4.36 \pm 0.32) \times 10^6$	1.00
Penciclovir		$(5.56 \pm 0.02) \times 10^6$	1.28
Guanine		$(3.92 \pm 0.02) \times 10^6$	0.90
Isocytosine		$(8.54 \pm 0.13) \times 10^4$	0.02
Imidazole		$(6.05 \pm 0.05) \times 10^6$	1.39

[a]k_{rel} is the rate constant for the substrates relative to acyclovir.

alkyl groups had a faster bimolecular reaction rate constant with $^1O_2$.

Further, the intermediates of acyclovir and penciclovir were also identified to support the conclusions; however, only 1 product with a mass-to-charge ratio of 158 (the chromatograms and MS fragmentation patterns are shown in Supplemental Data, Figures S8 and S9, respectively) was identified as 2,5-diamino-6-(hydroxyamino) pyrimidin-4-1 by LC-MS/MS.
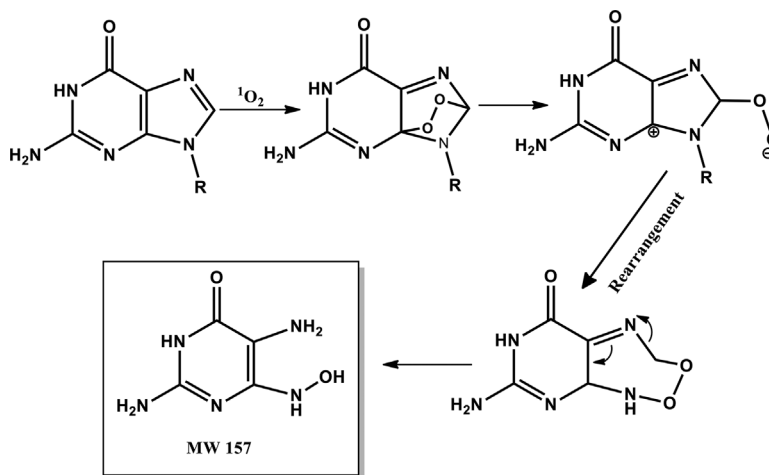
Figure 6 illustrates the proposed degradation pathway. The $^1O_2$ reacted with acyclovir or penciclovir, presumably through a Diels-Alder reaction at the imidazole substructural compound level, forming a zwitterionic intermediate. Then, the ether or alcohol side chain at the acyclovir or penciclovir molecule shifted, rearranging the imidazole structure, followed by a bond scission to form 1 product with a mass-to-charge ratio of 158. The results were consistent with the reaction site determination conclusion, further confirming that most of the $^1O_2$ reacted with the imidazole substructure. Other studies have demonstrated that $^1O_2$ reacts with imidazole to form an endoperoxide [38].

Ecotoxicity evolution

The results above demonstrate that $^1O_2$ oxidation was the main transformation pathway for the indirect photochemical transformation of acyclovir and penciclovir in fulvic acid–enriched water. As such, it is essential to assess the ecotoxicity of these $^1O_2$ oxidation products, as well as original compounds, during the photochemical transformation process. To do this, 3 different trophic level species, *P. phosphoreum*, *S. capricornutum*, and *D. magna*, were used to assess the acute ecotoxicity of the degradation solutions (Figure 7). *Photobacterium phosphoreum* (15 min), *S. capricornutum* (72 h), and *D. magna* (48 h) were inhibited by 12.6%, 9.3%, and 35.3% as a result of 0.1 mM acyclovir exposure and 14.4%, 10.5%, and 38.1% as a result of 0.1 mM penciclovir exposure, respectively. As degradation continues, acyclovir or penciclovir residual concentrations decrease rapidly, but there was also a slow increase in the treated solutions' inhibition efficiencies toward 3 species. When almost half of the acyclovir or penciclovir was eliminated after 120 min, the inhibition efficiencies of the degradation solution to *P. phosphoreum*, *S. capricornutum*, and *D. magna* remained, with 14.5%, 9.7%, and 53.2% for acyclovir and 16.5%, 11.0%, and 56.5% for penciclovir, respectively. An explanation for the increased toxicity could be that either higher toxic oxidation by-products, such as 2,5-diamino-6-(hydroxyamino) pyrimidin-4-1, were produced or the enhanced solubility of the transformation products led to increased exposure and subsequent enhanced critical body burdens in the target tissues of the test species. When the degradation time was extended to 180 min, a slight decrease was observed in the acute ecotoxicity of treated solutions. The decrease in the treated solution's inhibition efficiency with respect to *P. phosphoreum*, *S. capricornutum*, and *D. magna* was 10.7%, 5.2%, and 45.5% for acyclovir and
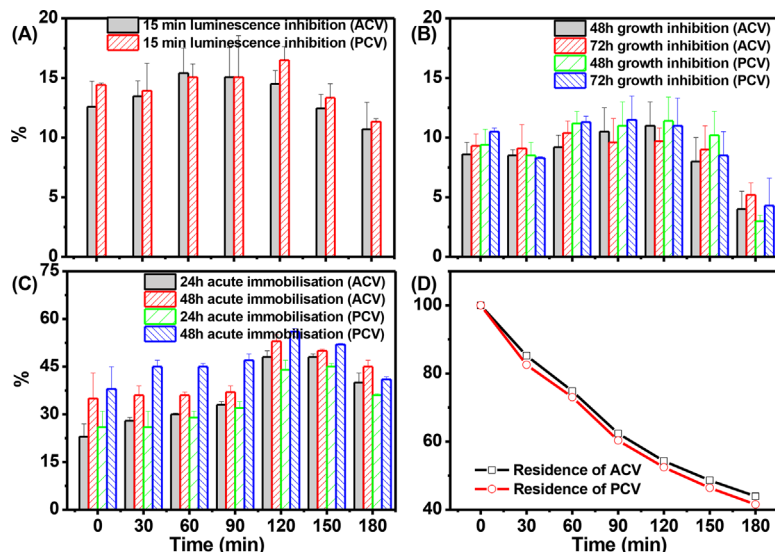

Figure 6. Proposed photochemical degradation pathways for the reaction of $^1O_2$ with acyclovir or penciclovir.

Figure 7. Evolution of the residence of acyclovir or penciclovir and the acute ecotoxicity evaluated with (**A**) *Photobacterium phosphoreum*, (**B**) *Selenastrum capricornutum*, and (**C**) *Daphnia magna* as well as (**D**) during the photochemical transformation of 100 μM substrates. Data are expressed as mean ± standard deviation; bars indicate standard deviation; $n = 3$. ACV = acyclovir; PCV = penciclovir.

11.3%, 4.3%, and 41.0% for penciclovir, respectively. In fact, the steady-state concentration of $^1O_2$ is only 10^{-13} M in natural water environments [39,40]; the bimolecular reaction rate constant between $^1O_2$ and substrates is only 6 orders of magnitude smaller than in the present experiment. That is, $^1O_2$ oxidation of acyclovir or penciclovir in natural water environments was very slow. As such, some ecological risk derived from the $^1O_2$ oxidation was only of slight consequence, whereas the indirect photochemical acyclovir or penciclovir transformations were dominated by the $^1O_2$ attack.

CONCLUSIONS

The present study provides a picture of the indirect photochemical transformation of acyclovir and penciclovir in water environments. Pharmaceutical loss under sunlight irradiation depends on chromophoric DOM sensitizer concentration. The $^1O_2$ molecule was the most important ROS involved in indirect photochemical degradation of these 2 antiviral drugs. The bimolecular reaction rate constants of acyclovir or penciclovir with ROS were measured to estimate their half-life in natural water environments and assess the risks to aquatic organisms.

As the dominant ROS, $^1O_2$ can attack acyclovir or penciclovir through the Diels-Alder reaction at the imidazole substructural level. The bimolecular reaction rate constants between the substructural guanine, isocytosine, and imidazole with $^1O_2$ were compared with original compounds to support the transformation mechanism. Finally, the ecotoxicity assessment of treated solutions shows that their photochemical transformation will result in some ecological risk in natural water environments, probably because of the slow photochemical transformation process.

REFERENCES

1. Halling-Sørensen B, Nors Nielsen S, Lanzky PF, Ingerslev F, Holten Lützhøft HC, Jørgensen SE. 1998. Occurrence, fate and effects of pharmaceutical substances in the environment—A review. *Chemosphere* 36:357–393.
2. Guardabassi L, Lo Fo Wong DMA, Dalsgaard A. 2002. The effects of tertiary wastewater treatment on the prevalence of antimicrobial resistant bacteria. *Water Res* 36:1955–1964.
3. Orlando EF, Kolok AS, Binzcik GA, Gates JL, Horton MK, Lambright CS, Gray LE, Soto AM, Guillette LJ. 2004. Endocrine-disrupting effects of cattle feedlot effluent on an aquatic sentinel species, the fathead minnow. *Environ Health Perspect* 112:353–358.
4. Cleuvers M. 2005. Initial risk assessment for three β-blockers found in the aquatic environment. *Chemosphere* 59:199–205.
5. Prasse C, Schlusener MP, Schulz R, Ternes TA. 2010. Antiviral drugs in wastewater and surface waters: A new pharmaceutical class of environmental relevance? *Environ Sci Technol* 44:1728–1735.
6. Mascolo G, Balest L, Cassano D, Laera G, Lopez A, Pollice A, Salerno C. 2010. Biodegradability of pharmaceutical industrial wastewater and formation of recalcitrant organic compounds during aerobic biological treatment. *Bioresour Technol* 101:2585–2591.
7. Brown SD, White CA, Chu CK, Bartlett MG. 2002. Determination of acyclovir in maternal plasma, amniotic fluid, fetal and placental tissues by high-performance liquid chromatography. *J Chromatogr B* 772:327–334.
8. Prasse C, Wagner M, Schulz R, Ternes TA. 2011. Biotransformation of the antiviral drugs acyclovir and penciclovir in activated sludge treatment. *Environ Sci Technol* 45:2761–2769.
9. Aldini G, Granata P, Orioli M, Santaniello E, Carini M. 2003. Detoxification of 4-hydroxynonenal (HNE) in keratinocytes: Characterization of conjugated metabolites by liquid chromatography/electrospray ionization tandem mass spectrometry. *J Mass Spectrom* 38:1160–1168.
10. Frischmann M, Bidmon C, Angerer J, Pischetsrieder M. 2005. Identification of DNA adducts of methylglyoxal. *Chem Res Toxicol* 18:1586–1592.
11. Ryan CC, Tan DT, Arnold WA. 2011. Direct and indirect photolysis of sulfamethoxazole and trimethoprim in wastewater treatment plant effluent. *Water Res* 45:1280–1286.
12. Luo X, Zheng Z, Greaves J, Cooper WJ, Song W. 2012. Trimethoprim: Kinetic and mechanistic considerations in photochemical environmental fate and AOP treatment. *Water Res* 46:1327–1336.
13. Boreen A, Arnold W, McNeill K. 2003. Photodegradation of pharmaceuticals in the aquatic environment: A review. *Aquat Sci* 65:320–341.

14. Cooper WJ, Zika RG, Petasne RG, Fischer AM. 1988. Sunlight-induced photochemistry of humic substances in natural waters: Major reactive species. In Suffet IH, MacCarthy P, eds, *Aquatic Humic Substances*, Vol 219, American Chemical Society, Washington, DC, pp 333–362.

15. Housari F, Vione D, Chiron S, Barbati S. 2010. Reactive photoinduced species in estuarine waters. Characterization of hydroxyl radical, singlet oxygen and dissolved organic matter triplet state in natural oxidation processes. *Photochem Photobiol Sci* 9:78–86.

16. Mill T. 1999. Predicting photoreaction rates in surface waters. *Chemosphere* 38:1379–1390.

17. Razavi B, Ben Abdelmelek S, Song W, O'Shea KE, Cooper WJ. 2011. Photochemical fate of atorvastatin (lipitor) in simulated natural waters. *Water Res* 45:625–631.

18. Kelly MM, Arnold WA. 2012. Direct and indirect photolysis of the phytoestrogens genistein and daidzein. *Environ Sci Technol* 46:5396–5403.

19. Zhou L, Ji Y, Zeng C, Zhang Y, Wang Z, Yang X. 2013. Aquatic photodegradation of sunscreen agent *p*-aminobenzoic acid in the presence of dissolved organic matter. *Water Res* 47:153–162.

20. Jacobs LE, Fimmen RL, Chin Y-P, Mash HE, Weavers LK. 2011. Fulvic acid mediated photolysis of ibuprofen in water. *Water Res* 45:4449–4458.

21. Mihas O, Kalogerakis N, Psillakis E. 2007. Photolysis of 2,4-dinitrotoluene in various water solutions: Effect of dissolved species. *J Hazard Mater* 146:535–539.

22. Carlos L, Mártire DO, Gonzalez MC, Gomis J, Bernabeu A, Amat AM, Arques A. 2012. Photochemical fate of a mixture of emerging pollutants in the presence of humic substances. *Water Res* 46:4732–4740.

23. An T, Fang H, Li G, Wang S, Yao S. 2014. Experimental and theoretical insights into photochemical transformation kinetics and mechanisms of aqueous propylparaben and risk assessment of its degradation products. *Environ Toxicol Chem* 33:1809–1816.

24. la Farre M, Perez S, Kantiani L, Barcelo D. 2008. Fate and toxicity of emerging pollutants, their metabolites and transformation products in the aquatic environment. *Trends Analyt Chem* 27:991–1007.

25. Hayase K, Tsubota H. 1985. Sedimentary humic-acid and fulvic-acid as fluorescent organic materials. *Geochim Cosmochim Acta* 49:159–163.

26. Tang WZ, Huang CP. 1996. 2,4-Dichlorophenol oxidation kinetics by fenton's reagent. *Environ Technol* 17:1371–1378.

27. Wang L, Xu H, Cooper WJ, Song W. 2012. Photochemical fate of beta-blockers in NOM enriched waters. *Sci Total Environ* 426:289–295.

28. Page SE, Arnold WA, McNeill K. 2010. Terephthalate as a probe for photochemically generated hydroxyl radical. *J Environ Monit* 12:1658–1665.

29. An TC, An JB, Gao YP, Li GY, Fang HS, Song WH. 2015. Photocatalytic degradation and mineralization mechanism and toxicity assessment of antivirus drug acyclovir: Experimental and theoretical studies. *Appl Catal B* 164:279–287.

30. Lin AYC, Wang XH, Lee WN. 2013. Phototransformation determines the fate of 5-fluorouracil and cyclophosphamide in natural surface waters. *Environ Sci Technol* 47:4104–4112.

31. Chen Y, Li H, Wang Z, Li H, Tao T, Zuo Y. 2012. Photodegradation of selected β-blockers in aqueous fulvic acid solutions: Kinetics, mechanism, and product analysis. *Water Res* 46:2965–2972.

32. Felcyn JR, Davis JCC, Tran LH, Berude JC, Latch DE. 2012. Aquatic photochemistry of isoflavone phytoestrogens: Degradation kinetics and pathways. *Environ Sci Technol* 46:6698–6704.

33. Merkel PB, Nilsson R, Kearns DR. 1972. Deuterium effects on singlet oxygen lifetimes in solutions. New test of singlet oxygen reactions. *J Am Chem Soc* 94:1030–1031.

34. Schweitzer C, Schmidt R. 2003. Physical mechanisms of generation and deactivation of singlet oxygen. *Chem Rev* 103:1685–1758.

35. An TC, An JB, Yang H, Li GY, Feng HS, Nie XP. 2011. Photocatalytic degradation kinetics and mechanism of antivirus drug-lamivudine in TiO$_2$ dispersion. *J Hazard Mater* 197:229–236.

36. Ge L, Chen J, Qiao X, Lin J, Cai X. 2009. Light-source-dependent effects of main water constituents on photodegradation of phenicol antibiotics: Mechanism and kinetics. *Environ Sci Technol* 43:3101–3107.

37. Wilkinson F, Helman WP, Ross AB. 1995. Rate constants for the decay and reactions of the lowest electronically excited singlet state of molecular oxygen in solution. An expanded and revised compilation. *J Phys Chem Ref Data* 24:663–677.

38. Kang P, Foote CS. 2002. Photosensitized oxidation of ^{13}C,^{15}N-labeled imidazole derivatives. *J Am Chem Soc* 124:9629–9638.

39. Haag WR, Hoigné J, Gassman E, Braun AM. 1984. Singlet oxygen in surface waters—Part I: Furfuryl alcohol as a trapping agent. *Chemosphere* 13:631–640.

40. Haag WR, Hoigne J. 1986. Singlet oxygen in surface waters. 3. Photochemical formation and steady-state concentrations in various types of waters. *Environ Sci Technol* 20:341–348.